PHYSICAL REVIEW B 92, 195135 (2015)

Temperature evolution of correlation strength in the superconducting state of high-T_c cuprates

S. Kudo,[1] T. Yoshida,[1] S. Ideta,[1] K. Takashima,[1] H. Anzai,[2] T. Fujita,[2] Y. Nakashima,[2] A. Ino,[2] M. Arita,[3] H. Namatame,[3] M. Taniguchi,[2,3] K. M. Kojima,[1] S. Uchida,[1] and A. Fujimori[1]
[1]*Department of Physics, University of Tokyo, Bunkyo-ku, Tokyo 113-0033, Japan*
[2]*Graduate School of Science, Hiroshima University, Higashi-Hiroshima 739-8526, Japan*
[3]*Hiroshima Synchrotron Center, Hiroshima University, Higashi-Hiroshima 739-0046, Japan*
(Received 8 August 2015; published 18 November 2015)

We have performed an angle-resolved photoemission study of the nodal quasiparticle spectra of the high-T_c cuprate trilayer $Bi_2Sr_2Ca_2Cu_3O_{10+\delta}$ ($T_c \sim 110$ K). The spectral weight Z of the nodal quasiparticle increases with decreasing temperature across T_c. Such a temperature dependence is qualitatively similar to that of the coherence peak intensity in the antinodal region of various high-T_c cuprates, although the nodal spectral weight remains finite and large above T_c. We attribute this observation to the reduction of electron correlation strength in going from the normal metallic state to the superconducting state, a characteristic behavior of a superconductor with strong electron correlation.

DOI: 10.1103/PhysRevB.92.195135 PACS number(s): 74.25.Jb, 74.72.Gh, 74.72.Kf

I. INTRODUCTION

The strength of electron correlation in a metal is represented by the renormalization factor $Z_{k_F} = |\langle \Phi_{k_F}(N-1)|a_{k_F}|\Phi_{k_F}(N)\rangle|^2$, where a_{k_F} is the annihilation operator of an electron on the Fermi surface, $\Phi_{k_F}(N)$ is the ground state, and $\Phi_{k_F}(N-1)$ is the lowest-energy state with a quasiparticle (QP) of momentum k_F. Z_{k_F} gives the weight of the QP peak in the single-particle spectral function $A(k,\varepsilon)$ at $k = k_F$ and ε at the Fermi level E_F, which can be measured by angle-resolved photoemission spectroscopy (ARPES) [1]. According to BCS theory, which describes superconductivity in metals with weak electron correlation, the QP is fully coherent ($Z_{k_F} = 1$) all over the Fermi surfaces, and in a d-wave BCS superconductor, the QP spectrum on the nodal point of the Fermi surface remains unchanged without gap opening and with $Z_{k_F} = 1$. One subtle change that has been noticed so far is the sharpening of the QP width below T_c (Ref. [2]). If superconductivity occurs in the presence of strong electron correlation, on the other hand, the nodal spectral weight increases in going from the normal state to the superconducting state as theoretically predicted by Chou, Lee, and Ho [3]. In the theory, the correlated normal state is represented by a projected Fermi liquid, and the correlated superconducting state is represented by a resonating valence bond (RVB) or a projected BCS state. The increase of the QP spectral weight Z_{k_F} reflects the partial recovery of the coherence from the highly incoherent projected Fermi-liquid state to the projected BCS state.

So far, the temperature dependence of the Drude weight in optical conductivity has been investigated for various cuprates [4–7]. In those studies, the low-energy electron number defined by the integration of optical conductivity below a certain cutoff frequency gradually increases with decreasing temperature. Such a behavior is also observed in normal metals such as gold, but the change in the cuprates, e.g., $La_{2-x}Sr_xCuO_4$ (LSCO), is more than one order of magnitude larger than that in gold. The optical conductivity can be expressed by a two-particle Green's function, and the QP spectral weight which is derived from the one-particle Green's function is also expected to show a similar temperature dependence. However, a direct test of the temperature dependence of the QP spectral weight has not been investigated in a systematic way. In the present work, we have performed an ARPES study of the trilayer cuprate superconductor $Bi_2Sr_2Ca_2Cu_3O_{10+\delta}$ (Bi2223) in a wide temperature range and investigated changes in the spectral weight of the nodal QP with temperature. The results indeed show a dramatic increase of the QP spectral weight with decreasing temperature.

II. EXPERIMENT

Single crystals of Bi2223 ($T_c = 110$ K) were grown using the traveling-solvent floating-zone (TSFZ) method. ARPES measurements were carried out at BL-9A of the Hiroshima Synchrotron Radiation Center (HiSOR). Incident photons have an energy of $h\nu = 7.56$ eV, and measurements were made at $T = 11, 90, 120$, and 160 K. A SCIENTA SES-R4000 analyzer was used in the angle mode with a total energy and momentum resolution of $\sim$5 meV and $\sim$0.3°, respectively. All the samples were cleaved *in situ* under an ultrahigh vacuum of 10^{-11} Torr. The position of E_F was calibrated with gold spectra.

III. RESULTS AND DISCUSSION

A. Z_{k_F} deduced from MDCs

The single-particle spectral function $A(\mathbf{k},\varepsilon)$ measured by ARPES is the imaginary part of the single-particle Green's function $G(\mathbf{k},\varepsilon) \equiv 1/[\varepsilon - \varepsilon_\mathbf{k} - \Sigma(\mathbf{k},\varepsilon)]$:

$$A(\mathbf{k},\varepsilon) \equiv -\frac{1}{\pi}\mathrm{Im}G = -\frac{1}{\pi}\frac{\mathrm{Im}\Sigma(\mathbf{k},\varepsilon)}{[\varepsilon - \varepsilon_\mathbf{k} - \mathrm{Re}\Sigma(\mathbf{k},\varepsilon)]^2 + [\mathrm{Im}\Sigma(\mathbf{k},\varepsilon)]^2}, \quad (1)$$

where $\varepsilon_\mathbf{k}$ is the bare-band electron energy with momentum $\mathbf{k}$ and $\Sigma(\mathbf{k},\varepsilon)$ is the self-energy. $\varepsilon = 0$ is chosen at E_F. The pole of $\mathrm{Re}G(\mathbf{k},\varepsilon)$, $\varepsilon = \varepsilon^*_\mathbf{k}$, is determined by the equation $\varepsilon - \varepsilon_\mathbf{k} - \mathrm{Re}\Sigma(\mathbf{k},\varepsilon) = 0$, and the residue of the pole

$$Z_\mathbf{k}(\varepsilon^*_\mathbf{k}) \equiv \left(1 - \left.\frac{\partial \mathrm{Re}\Sigma(\mathbf{k},\varepsilon)}{\partial\varepsilon}\right|_{\varepsilon=\varepsilon^*_\mathbf{k}}\right)^{-1} (<1) \quad (2)$$

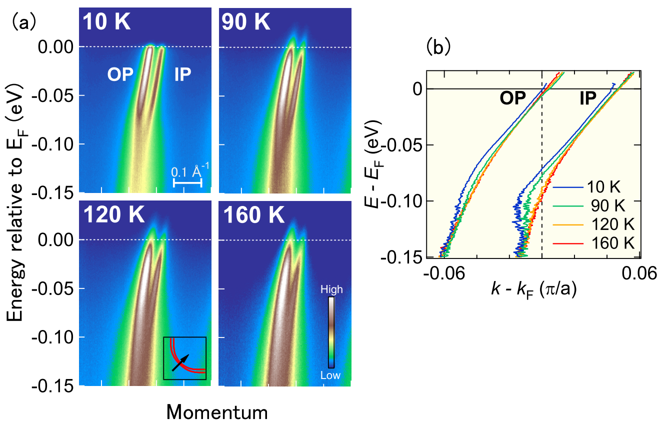

FIG. 1. (Color online) ARPES spectra of Bi2223 in the nodal direction at various temperatures. (a) Intensity plots in energy-momentum space along the nodal direction (see the inset to the 120 K data). OP and IP denote the outer and inner quasiparticle bands, respectively. (b) Quasiparticle (QP) band dispersions for the IP and OP bands deduced from the MDC peak positions.

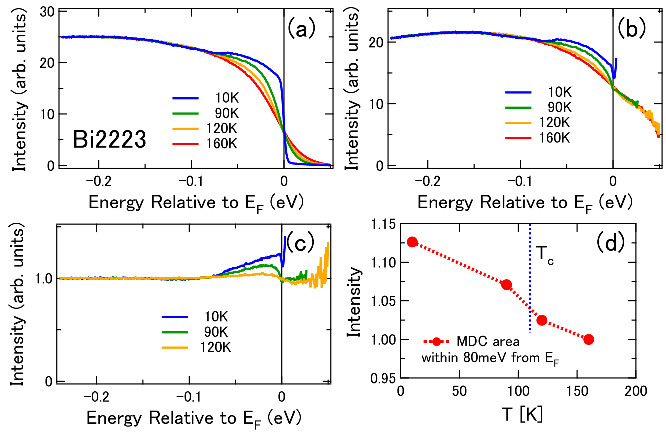

FIG. 2. (Color online) ARPES spectra of Bi2223 integrated along the nodal direction including both the IP and OP bands. (a) Raw data. (b) Spectra divided by the Fermi-Dirac function. (c) Spectra in (b) divided by the spectrum at 160 K. (d) Temperature dependence of the spectral weight intensity within 80 meV from E_F (normalized to the 160 K data).

gives the spectral weight of the QP. In the vicinity of $\varepsilon = \varepsilon^*_{\mathbf{k}}$, one can expand $\mathrm{Re}\Sigma(\mathbf{k},\varepsilon)$ as

$$\mathrm{Re}\Sigma(\mathbf{k},\varepsilon) \simeq \mathrm{Re}\Sigma(\mathbf{k},\varepsilon^*_{\mathbf{k}}) + \left.\frac{\partial \mathrm{Re}\Sigma(\mathbf{k},\varepsilon)}{\partial \varepsilon}\right|_{\varepsilon=\varepsilon^*_{\mathbf{k}}} (\varepsilon - \varepsilon^*_{\mathbf{k}})$$
$$\simeq \varepsilon - \varepsilon_{\mathbf{k}} - \frac{1}{Z_{\mathbf{k}}(\varepsilon^*_{\mathbf{k}})}(\varepsilon - \varepsilon^*_{\mathbf{k}}). \tag{3}$$

In the vicinity of E_F, $\varepsilon^*_{\mathbf{k}} \sim v^*_{\mathbf{k}}(k - k_F)$, where k is taken perpendicular to the Fermi surface and $v^*_{\mathbf{k}_F}(\equiv |\nabla \varepsilon^*_{\mathbf{k}_F}|)$ is the Fermi velocity. Then, the momentum distribution curve (MDC) at E_F is given by

$$A(\mathbf{k},0) \simeq -\frac{Z_{\mathbf{k}_F}(0)/v^*_{\mathbf{k}_F}}{\pi} \frac{Z_{\mathbf{k}_F}(0)\mathrm{Im}\Sigma(\mathbf{k},0)/v^*_{\mathbf{k}_F}}{(k-k_F)^2 + (Z_{\mathbf{k}_F}(0)\mathrm{Im}\Sigma(\mathbf{k},0)/v^*_{\mathbf{k}_F})^2}. \tag{4}$$

This MDC is a Lorentzian if the self-energy $\Sigma(\mathbf{k},\varepsilon)$ is not strongly dependent on k perpendicular to the Fermi surface. The QP weight is therefore given by

$$Z_{k_F}(0) = \int_{-\infty}^{\infty} A(\mathbf{k},0)d\mathbf{k} \times v^*_{\mathbf{k}_F}. \tag{5}$$

Figure 1(a) shows plots of spectral intensities along the nodal $\mathbf{k} = (0,0) - (\pi,\pi)$ cut. There are two bands corresponding to the inner CuO_2 plane (IP) and outer CuO_2 plane (OP) of the trilayer cuprate [8]. In Fig. 1(b), the QP dispersions are traced by the peak positions of the MDCs. One can clearly see kinks in the QP dispersions which show temperature dependences. From these spectra, we shall deduce the temperature dependence of the QP spectral weight Z_{k_F} in the nodal direction.

First, we look into the temperature dependence of the MDC area, namely, the momentum-integrated ARPES spectra along the nodal direction, as shown in Fig. 2(a). Here, the intensity has been normalized to the intensity at high binding energies >0.2 eV. Figure 2(b) shows the same data divided by the Fermi-Dirac (FD) function (The gap opens in the 10 K data because the cut was slightly off nodal due to small misalignment). In order to emphasize changes induced by superconductivity, the spectra in Fig. 2(b) have been divided by the 160 K spectrum and are shown in Fig. 2(c). Thus obtained spectra clearly indicate that the intensity within 80 meV of E_F increases with decreasing temperature. The integrated intensities within ~80 meV are plotted as a function of temperature in Fig. 2(d). Note that the integrated spectral intensities include signals from both the IP and OP bands.

In order to estimate the QP spectral weight $Z_{k_F}(0)$ at E_F using Eq. (5), signals from the IP and OP bands have to be separated. For that purpose, the MDC at each energy has been fitted to two Lorentzians. The Fermi velocity at E_F, v^*_F, has been obtained from the slope of the QP dispersion shown in Fig. 1(b). Here, we extend Eq. (5), which is defined at E_F, to finite energies as $Z_{kF}(\varepsilon)f(\varepsilon) \propto \int_{-\infty}^{\infty} A(\mathbf{k},\varepsilon)d\mathbf{k} \times v_k(\varepsilon)$. The momentum-integrated spectrum for each of the IP and OP bands at various temperatures is plotted in Figs. 3(a) and 3(b). Since the observed MDC area is $f(\varepsilon)\int_{-\infty}^{\infty} A(\mathbf{k},\varepsilon)d\mathbf{k}$, where $f(\varepsilon)$ is the FD distribution function, we have divided the spectra by the FD function as plotted in Figs. 3(c) and 3(d). The $Z_{k_F}(\varepsilon)$ spectra thus deduced using the finite-energy version of Eq. (5) plotted in Figs. 3(e) and 3(f).

$Z_{k_F}(\varepsilon)$ at $T = 10$ K is nearly constant in the displayed energy range near E_F as expected for a Fermi liquid or a QP at the node of a d-wave BCS superconductor, while $Z(\varepsilon)$ at high temperatures (120 K and 160 K) decrease towards E_F and above it. Also, the $Z_{k_F}(0)$ value at E_F itself decreases with increasing temperature. This indicates that the nodal spectrum is highly coherent well below T_c but gradually becomes incoherent with increasing temperature. The degree of deviation from constant $Z_{k_F}(\varepsilon)$ or the loss of coherence is a little stronger for the IP band than the OP band, probably due to the smaller hole concentration and hence the stronger electron correlation in the IP band [8].

B. Z_{k_F} deduced from EDCs

Although less accurate, the spectral weight Z_{k_F} can also be derived from energy distribution curves (EDCs), under the

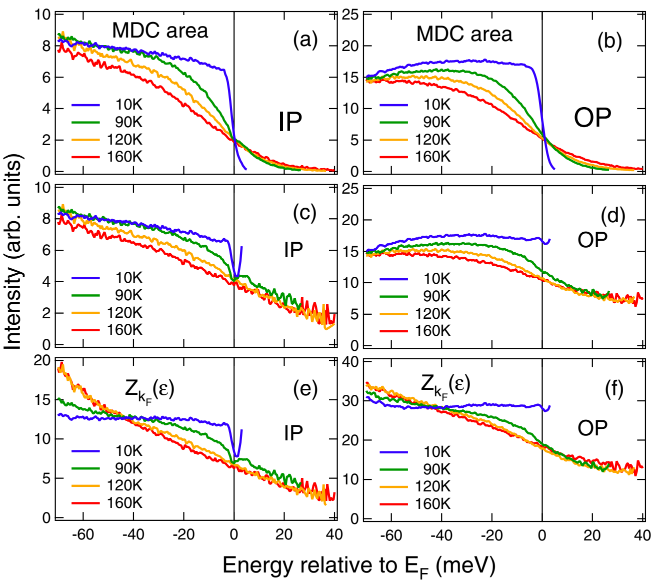

FIG. 3. (Color online) Spectral weight $Z_{k_F}(\varepsilon)$ for the IP and OP bands of Bi2223 deduced from the MDC peak area and the QP velocity $v_k^*(\varepsilon)$. In order to extract the MDC area for the IP and OP bands separately, MDC data in Fig. 1 were fitted to two Lorentzians. (a) and (b) MDC area with the same intensity normalization as Fig. 2. (c) and (d) MDC area divided by the Fermi-Dirac function convoluted with a Gaussian. (e) and (f) $Z_{k_F}(\epsilon) = \int_{-\infty}^{\infty} A(\mathbf{k},0)d\mathbf{k} \times v_k^*(\varepsilon)$, where $v_k^*(\varepsilon)$ has been deduced from the slope of the QP dispersions shown in Fig. 1(b). The dip at E_F in the 10 K data, particularly for the IP band, arises because the cut direction was slightly off node due to small misalignment.

assumption that the normal state is a Fermi liquid (although the high-T_c cuprates near optimum doping are considered to be a marginal Fermi liquid [9]). For a Fermi liquid, $\Sigma(\mathbf{k},\varepsilon)$ can be expanded in the vicinity of E_F as

$$\Sigma(\mathbf{k},\varepsilon) \simeq -\alpha_{\mathbf{k}}\varepsilon - i\beta_{\mathbf{k}}\varepsilon^2 \; (\alpha_{\mathbf{k}},\, \beta_{\mathbf{k}} > 0). \tag{6}$$

From Eqs. (1) and (6), therefore, one obtains

$$\begin{aligned} A(\mathbf{k},\varepsilon) &\simeq \frac{1}{\pi}\frac{\beta_{\mathbf{k}}\varepsilon^2}{(\varepsilon - \varepsilon_{\mathbf{k}} + \alpha_{\mathbf{k}}\varepsilon)^2 + (\beta_{\mathbf{k}}\varepsilon^2)^2} \\ &= \frac{Z_{\mathbf{k}}}{\pi}\frac{Z_{\mathbf{k}}\beta_{\mathbf{k}}\varepsilon^2}{\left(\varepsilon - Z_{\mathbf{k}}\varepsilon_{\mathbf{k}}^0\right)^2 + (Z_{\mathbf{k}}\beta_{\mathbf{k}}\varepsilon^2)^2}, \end{aligned} \tag{7}$$

where $Z_{\mathbf{k}} \equiv (1+\alpha_{\mathbf{k}})^{-1}$ (<1). When $\mathbf{k}$ is not on the Fermi surface ($\mathbf{k} \neq \mathbf{k}_F$), in the vicinity of E_F,

$$A(\mathbf{k},\varepsilon) \simeq \frac{\beta_{\mathbf{k}}}{\pi}\frac{\varepsilon^2}{\varepsilon_{\mathbf{k}}^2} \propto -\mathrm{Im}\Sigma(\mathbf{k},\varepsilon), \tag{8}$$

and therefore, there is no spectral weight at E_F. As $\mathbf{k}$ approaches the Fermi surface, the QP peak width becomes narrow, and when $\mathbf{k}$ is on the Fermi surface ($\mathbf{k} = \mathbf{k}_F$), the QP peak becomes a δ function $Z_{\mathbf{k}}\delta(\varepsilon)$:

$$A(\mathbf{k}_F,\varepsilon) \simeq Z_k\delta(\varepsilon) + \frac{Z_{\mathbf{k}_F}}{\pi}\frac{Z_{\mathbf{k}_F}\beta_{\mathbf{k}_F}}{1 + Z_{\mathbf{k}_F}^2\beta_{\mathbf{k}_F}^2\varepsilon^2}. \tag{9}$$

That is, the line shape of the EDC at $\mathbf{k} = \mathbf{k}_F$ is a δ function superposed on top of a broad Lorentzian-like background, with both centered at E_F [10]. Here, the δ function is broadened into a Lorentzian due to impurity scattering. Experimentally, therefore, we expect to observe two overlapping Lorentzians with narrow and broad widths.

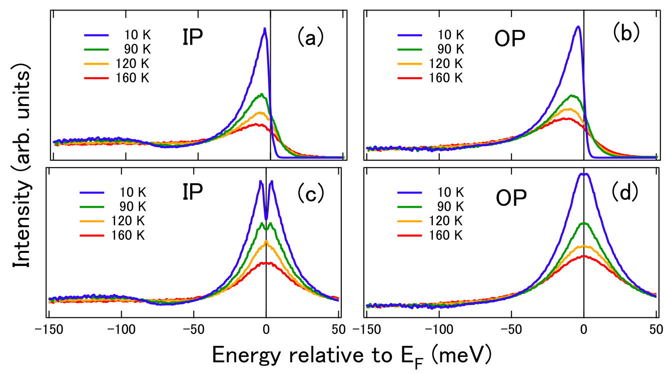

FIG. 4. (Color online) EDCs of Bi2223 at k_F on the node. (a) and (b) Temperature dependence of the EDCs at k_F. (c) and (d) Symmetrized EDCs at k_F. The area of the Lorentzian centered at E_F gives $Z(0)$.

Figure 4 shows EDCs at $k = k_F$ [Figs. 4(a) and 4(b)] and their symmetrized spectra [Figs. 4(c) and 4(d)]. As shown in Figs. 4(c) and 4(d) for the IP and OP bands, the line shape of each symmetrized spectrum shows a Lorentzian-like central peak. (The splitting of the symmetrized 10 K data at E_F, particularly in the IP data, arises from small misalignment of the nodal direction.) Again, the increase of the spectral weight of the central peak is seen with decreasing temperature. According to Eq. (12), a broad Lorenztian-like background is expected in addition to the relatively sharp Lorentzian QP peak of spectral weight $Z_{k_F}(0)$. However, because such a background feature appears negligibly small, we have estimated $Z_{k_F}(0)$ from the area of the symmetrized EDCs within 80 meV of E_F.

C. Temperature dependence of Z_{k_F}

The temperature dependence of the nodal spectral weight $Z_{k_F}(0)$ for the IP and OP bands obtained from the MDC and EDC analysis is summarized in Fig. 5. The values of $Z_{k_F}(0)$ at various temperatures have been normalized to the values at 160 K. The temperature dependence of Z_{k_F} obtained by the MDCs and EDCs falls almost on the same curve. The results show a clear increase of Z_{k_F} by as much as ~50% in going from 160 to 10 K. The Z_{k_F} of the IP band increases a little more rapidly than that of the OP band with decreasing temperature, consistent with the prediction by Chou *et al.* [3]. Because the IP and OP bands are underdoped and overdoped, respectively, the result indicates that the underdoped CuO_2 plane loses coherence faster than the overdoped CuO_2 plane with temperature. Here, we have also plotted $Z_{k_F}(0)$ of Bi2212 in Ref. [11]. The Bi2212 data also show a similar temperature dependence to that of Bi2223. The smaller increase in the Z_{k_F} of Bi2212 with decreasing temperature than that in Bi2223 may reflect the smaller superconducting order parameter.

A similar increase of the low-energy spectral weight has been observed in optical conductivity [4–7], indicating an increase of the coherence in the superconducting state

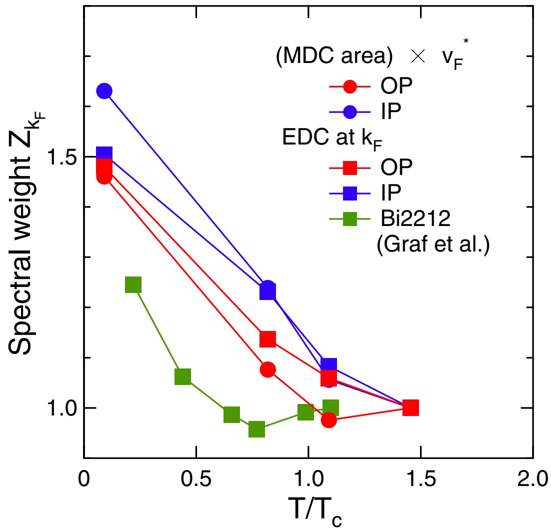

FIG. 5. (Color online) Spectral weight at E_F, $Z_{k_F}(0)$, for the OP and IP bands of Bi2223 derived from MDCs and EDCs (under the assumption of a Fermi liquid) plotted as functions of temperature. $Z_{k_F}(0)$ for Bi2212 ($T_c = 91$ K) deduced from the EDCs in Ref. [11] is also plotted.

compared to the normal state. In the underdoped region, the Drude weight of the high-T_c cuprates shows a strong temperature dependence compared to that in the overdoped region, which can be interpreted as an electron correlation and/or pseudogap effects [7,12]. Particularly in the underdoped region, the low-energy spectral weight, i.e., the electron kinetic energy, strongly increases below T_c [13]. Since the contribution from the kinetic energy to the condensation energy is significant compared to the conventional superconductors, kinetic-energy-driven superconductivity has been proposed [14,15]. The increase in the spectral weight below T_c is up to 50%, which is much larger than the change in the Drude weight in various high-T_c cuprates. Such a strong increase of the spectral weight, and hence the increase in the kinetic energy, may be one of the reasons for the very high T_c in the trilayer cuprates. Since correlation between the antinodal spectral weight and superfluid density (SFD) has been discussed in previous ARPES studies [16,17], one may expect a similar relationship between the nodal spectral weight Z_F and SFD. However, we have not found a theoretical connection between them so far, and the SFD is rather correlated with the Fermi arc length [18]. If there were phase separation into the superconducting and nonmetallic phases, correlation between the SFD and the nodal Z_F would exist.

As shown in Figs. 3(e) and 3(f), $Z(\varepsilon)$ below T_c shows a nearly energy independent Fermi-liquid-like behavior, which is in contrast to strongly energy dependent incoherent behavior above T_c. Particularly, $Z(\varepsilon)$ of IP monotonically decrease with energy, indicating a strongly incoherent nature of the spectral weight. In previous photoemission studies, the coherence temperature T_{coh} was deduced from the line shape of the spectra [19,20] and was found to increase monotonically with hole concentration, consistent with the prediction of the t-J model. In the present result, even though the nodal spectral weight is most coherent on the Fermi surface, the spectra become highly incoherent at high temperatures, also consistent with the RVB picture based on the t-J model.

IV. CONCLUSION

We have performed a temperature-dependent angle-resolved photoemission spectroscopy study of the optimally doped trilayer high-T_c cuprates Bi2223 to investigate the temperature dependence of spectral weight Z_{k_F} in the nodal direction. In contrast to what is expected from BCS theory, all the results show an increase of spectral weight Z_{k_F} with decreasing temperature below T_c, consistent with the theoretical prediction on correlated superconductors [3], and suggest a transition from the relatively incoherent metal to the relatively coherent superconductor across T_c. The result indicates not only the change in the coherence at T_c but also the rapid evolution of the coherence with decreasing temperature below T_c.

ACKNOWLEDGMENTS

We are thankful for fruitful and enlightening discussions with T. K. Lee, C. M. Ho, and C. P. Chou. ARPES experiments were carried out at HiSOR (Proposals No. 07-A-10 and No. 08-A-35).

[1] S. Hüfner, *Photoelectron Spectroscopy*, 3rd ed. (Springer, Berlin, 2003).
[2] T. Yamasaki, K. Yamazaki, A. Ino, M. Arita, H. Namatame, M. Taniguchi, A. Fujimori, Z.-X. Shen, M. Ishikado, and S. Uchida, Phys. Rev. B **75**, 140513 (2007).
[3] C. P. Chou, T. K. Lee, and C. M. Ho, J. Phys. Chem. Solids **69**, 2993 (2008).
[4] F. Carbone, A. B. Kuzmenko, H. J. A. Molegraaf, E. van Heumen, V. Lukovac, F. Marsiglio, D. van der Marel, K. Haule, G. Kotliar, H. Berger, S. Courjault, P. H. Kes, and M. Li, Phys. Rev. B **74**, 064510 (2006).
[5] M. Ortolani, P. Calvani, and S. Lupi, Phys. Rev. Lett. **94**, 067002 (2005).
[6] J. Hwang, J. Yang, T. Timusk, S. G. Sharapov, J. P. Carbotte, D. A. Bonn, R. Liang, and W. N. Hardy, Phys. Rev. B **73**, 014508 (2006).
[7] N. Bontemps, Physica C (Amsterdam, Neth.) **460-462**, 162 (2007).
[8] S. Ideta, K. Takashima, M. Hashimoto, T. Yoshida, A. Fujimori, H. Anzai, T. Fujita, Y. Nakashima, A. Ino, M. Arita, H. Namatame, M. Taniguchi, K. Ono, M. Kubota, D. H. Lu, Z.-X. Shen, K. M. Kojima, and S. Uchida, Phys. Rev. Lett. **104**, 227001 (2010).
[9] C. M. Varma, P. B. Littlewood, S. Schmitt-Rink, E. Abrahams, and A. E. Ruckenstein, Phys. Rev. Lett. **63**, 1996 (1989).
[10] J. W. Allen, G.-H. Gweon, R. Claessen, and K. Matho, J. Phys. Chem. Solids **56**, 1849 (1995).

[11] J. Graf, C. Jozwiak, C. L. Smallwood, H. Eisaki, R. A. Kaindl, D.-H. Lee, and A. Lanzara, Nat. Phys. **7**, 805 (2011).

[12] A. F. Santander-Syro, R. P. S. M. Lobo, N. Bontemps, W. Lopera, D. Giratá, Z. Konstantinovic, Z. Z. Li, and H. Raffy, Phys. Rev. B **70**, 134504 (2004).

[13] H. J. A. Molegraaf, C. Presura, D. van der Marel, P. H. Kes, and M. Li, Science **295**, 2239 (2002).

[14] T. A. Maier, M. Jarrell, A. Macridin, and C. Slezak, Phys. Rev. Lett. **92**, 027005 (2004).

[15] M. R. Norman, A. Kaminski, J. Mesot, and J. C. Campuzano, Phys. Rev. B **63**, 140508 (2001).

[16] D. L. Feng, D. H. Lu, K. M. Shen, C. Kim, H. Eisaki, A. Damascelli, R. Yoshizaki, J.-i. Shimoyama, K. Kishio, G. D. Gu, S. Oh, A. Andrus, J. O'Donnell, J. N. Eckstein, and Z.-X. Shen, Science **289**, 277 (2000).

[17] H. Ding, J. R. Engelbrecht, Z. Wang, J. C. Campuzano, S.-C. Wang, H.-B. Yang, R. Rogan, T. Takahashi, K. Kadowaki, and D. G. Hinks, Phys. Rev. Lett. **87**, 227001 (2001).

[18] T. Yoshida, X. J. Zhou, D. H. Lu, S. Komiya, Y. Ando, H. Eisaki, T. Kakeshita, S. Uchida, Z. Hussain, Z.-X. Shen, and A. Fujimori, J. Phys. Condens. Matter **19**, 125209 (2007).

[19] A. Kaminski, S. Rosenkranz, H. M. Fretwell, Z. Z. Li, H. Raffy, M. Randeria, M. R. Norman, and J. C. Campuzano, Phys. Rev. Lett. **90**, 207003 (2003).

[20] M. Hashimoto, T. Yoshida, K. Tanaka, A. Fujimori, M. Okusawa, S. Wakimoto, K. Yamada, T. Kakeshita, H. Eisaki, and S. Uchida, Phys. Rev. B **79**, 140502 (2009).